Stable Long-Term Retrieval of Tropospheric Temperature Time Series from the Microwave Sounding Unit

Matthias C. Schabel, Carl A. Mears, and Frank J. Wentz
Remote Sensing Systems
438 First St. Suite 200
Santa Rosa, CA 95401

Climatological time-series of tropospheric temperatures from the Microwave Sounding Unit (MSU) are potentially of great value in validating observations of climate change due to their excellent spatial and temporal coverage. However, the long-term trend signal is small relative to natural seasonal and inter-annual variability and inter-satellite biases, and is comparable to diurnal temperature drift arising from variation of the satellite local crossing time. Additional effects due to time-varying non-linear instrument response also contribute to instrument error. We discuss a consistent methodology for compensating for these factors and present an error model quantifying their significance in determination of long-term trends.

I. INTRODUCTION

The high temporal and spatial resolution provided by satellite observations makes them attractive for climate change monitoring purposes. For these applications, the MSU is particularly interesting because it is a nearly direct proxy measure of layer averaged atmospheric temperature over a period spanning nearly 25 years with minimal instrumentation changes [1,2,3]. Accurate determination of long-term temperature trends in the troposphere is a difficult and complex task due to the small size of the trend signal relative to natural seasonal and interannual variability and to the presence of other time-varying biases which can alias a false signal into the true trend. The high level of interest in the MSU data and the discovery of undetected errors in a previous analysis of this data [1] has encouraged us to undertake a complete and independent reanalysis of this data set.

II. COMPUTING BRIGHTNESS TEMPERATURE

Implicit in any effort to produce a merged series of brightness temperature observations from multiple instruments is the development of an analysis methodology that provides self-consistent and quality-controlled results for each individual instrument. This methodology is given schematically in the form of the flowchart in Fig. 1. We begin from the unprocessed (Level 0) raw count data, checking all swaths within an orbit for basic consistency and quality control and verifying that their time-ordering is correct. Observations from known periods during which the instrument function was compromised are then removed, and instrument calibration coefficients are extracted.

Earlier work revealing satellite orbit decay to be a significant source of error in the MSU 2LT product derived from differencing near-nadir and near-limb observations [1] led us to implement an extensive geolocation validation system. Utilizing two-line orbital elements (TLEs) provided by the US Space Command [4] and a highly accurate orbit propagation model [5], we independently recomputed the satellite geolocation and orbit height, revealing significant errors (up to 30km) in reported heights prior to September 1994. Instances where the reported subtrack geolocation differs from that predicted by more than 100km are flagged suspect, as are nadir angles which differ from nominal by more than 1 degree.

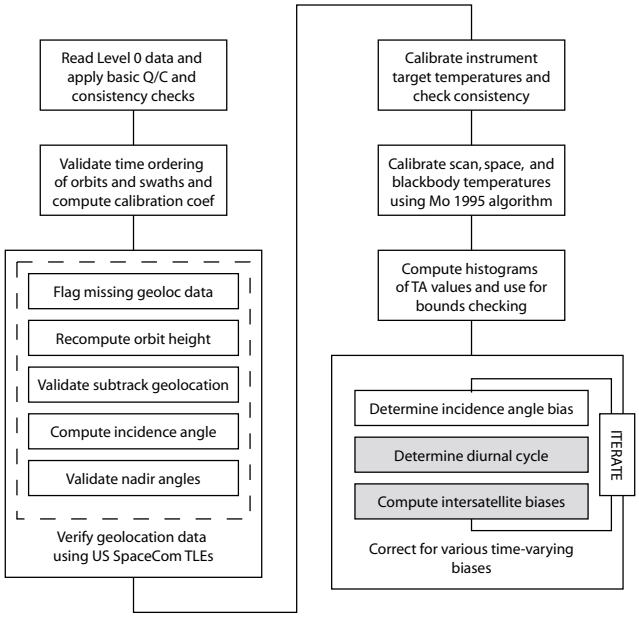

Fig. 1. Flowchart detailing steps involved in production of a climatological merged time-series of MSU tropospheric temperature observations. Of the various steps in this analysis, the two highlighted in gray are critical to accurate computation of long-term trends in this data set. In this paper we focus on inter-satellite merging, error propagation, and sensitivity analysis. Details of the diurnal cycle determination are presented in [9].

0-7803-7537-8/02/$17.00 (C) 2002 IEEE

Once geolocation validation is complete, the instrument target temperatures are calibrated and checked for consistency, and scan, space, and blackbody counts are converted to brightness temperatures (TB) using an algorithm by Mo, *et al*., [6] which corrects for nonlinearities in the instrument response to second order in target temperature. Histograms of the target temperatures and TBs are computed for each instrument, and are used to identify outlier cutoffs for further quality control.

The final sequence of steps iteratively determines corrections for three interconnected time-dependent biases. Slight imprecision in the alignment of various components of the MSU instruments manifests itself in the appearance of cross-track biases in which nominally equivalent field of view (FOV) pairs display a consistent TB differential due to differences in the resulting earth incidence angle. This roll error is quantified by constructing zonal monthly time-series of the TB differences for the five distinct FOV pairs. Climatological atmospheric profiles from the NCEP climate model reanalysis are combined with a sophisticated model of ocean surface emissivity [7] to compute the partial derivative of brightness temperature with incidence angle near the nominal values

$$\frac{\partial T_B}{\partial \theta}_{\theta \sim \theta_i}, \tag{1}$$

from which the effect of satellite roll on TB may be simulated. Regression of the measured cross-track biases to the model simulations enables us to determine the time-varying satellite roll, which is more than 1 degree in the case of some of the earliest instruments. This roll error is combined with incidence angle variation arising from fluctuating satellite orbital altitude, with the model data used to compute corrections to the brightness temperatures to achieve fixed effective incidence angle along with corresponding limb corrections to compensate for TB variation across the swath [8].

A second time-varying bias in the MSU data arises from the existence of a diurnal cycle in both the surface and, to a lesser extent, atmospheric temperatures. Unlike the roll bias, which is invariant between ascending and descending passes, the diurnal signal changes sign between ascending and descending passes depending on whether the crossing time is in the morning or afternoon. Due to slow drifts in the local equator crossing times of the various NOAA polar orbiters, a corresponding slow drift is introduced by the changing amplitude of the diurnal cycle over the course of the day. The extraction of this small effect is complex, but is necessary in order to achieve the high stability required for climate change applications. Details of the procedure for quantifying diurnal bias are presented in [9], with the results used to correct all observations to a single effective local crossing time.

Finally, once each individual instrument has been calibrated and corrected for the various biases discussed above, data from the nine independent instruments must be merged and error bounds established on the stability of the resulting time-series.

III. MERGING SERIES FROM MULTIPLE SATELLITES

Uncorrected residual biases between instruments are large relative to the small (tenths of K per decade) temperature trends we would like to measure. For this reason, the individual time-series of brightness temperature resulting from the quality control and calibration procedure discussed in Sec. II must be merged to remove inter-satellite offsets. Furthermore, a measurable residual nonlinearity of uncertain origin appears in the form of remnant correlations between measured TB and the hot calibration target temperature [3]. This so-called "instrument body effect" may arise from incomplete compensation for radiometer nonlinearity, or may represent spillover into the antenna from some other part of the satellite, or may arise from other unknown factors. It appears, however, to be sufficiently well-modeled by a linear correction, so that errors in the MSU TBs can be represented by

$$\vec{T}_{B,i} = \vec{T}_0 + \Delta T_{B,i} + \alpha_i \vec{T}_{T,i} + \vec{\varepsilon}_i, \tag{2}$$

where $\vec{T}_{B,i}$ is the vector of measured TBs for instrument i, $\vec{T}_0$ is the actual "true" tropospheric temperature, $\Delta T_{B,i}$ is the constant offset for instrument i, $\alpha_i \vec{T}_{T,i}$ is the product of a (hopefully) small "target factor" describing the correlation between the measured temperature and the residual temperature of the hot load after subtraction of its mean, and $\vec{\varepsilon}_i$ is a vector of residual noise which should be uncorrelated if the model in Eq. 2 is adequate.

Because of the significantly larger diurnal cycle and higher variability of land surface emissivity with changes in surface moisture, snow cover, vegetation, and other difficult to characterize factors, we restrict our merging analysis to data over oceans only, and further limit ourselves to observations in the range of latitudes from 50S to 50N to exclude high latitude regions with large synoptic variability and uneven spatiotemporal sampling. Cosine-weighted global pentad averages of incidence-angle-, and diurnally corrected TBs for the limb-corrected central 5 FOVs for each instrument were generated, with pentads having fewer than 95% of the median number of samples per pentad being discarded to further minimize sampling variability.

The resulting series were then separated into linearly independent time intervals in which two or more (at most three) satellites made simultaneous observations. NOAA-10 was chosen to be the arbitrary reference instrument with zero bias as it was quite stable over its lifetime, with little diurnal drift and a minimal roll bias. For each overlap pentad, Eq. 2 was differenced, leading to a system of ~1200 equations in 17 (8 offsets + 9 target factors) unknowns to be solved by linear regression. Fig. 2 shows a typical pentad series for the overlap between NOAA-11 and NOAA-12 and the corresponding regression.

0-7803-7537-8/02/$17.00 (C) 2002 IEEE

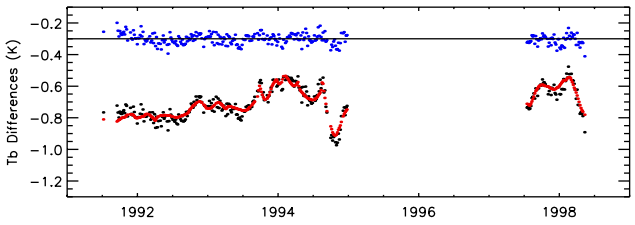

Fig. 2. A plot of pentad-averaged inter-satellite differences (black), bias and target factor regression (red), and fit residuals (blue) for the series of overlapping observations for NOAA-11 and NOAA-12.

IV. Error Analysis and Sensitivity

As we are primarily interested in the low-frequency behavior of tropospheric temperature, we focus here on errors in the secular linear trend in brightness temperature for the entire global merged time-series, as shown in Fig. 3. This is formed by averaging the pentad data for all satellites, corrected using the offsets and target factors from the regression in Sec. III, and median filtered with a 5-pentad window to eliminate outliers to which the trend estimate is especially sensitive.

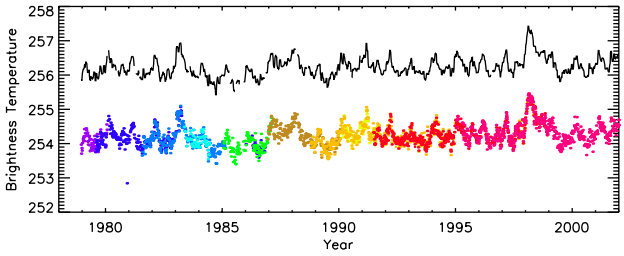

Fig. 3. Merged global ocean-only MSU TB pentad time series through the end of 2001. Data from individual satellites are shown in color in the lower curve, offset by 2K for clarity, while the upper curve is the final merged series, filtered by a 5 pentad moving average median filter.

The primary error source to be considered is the sensitivity of the long-term trend to uncertainties in the biases and target factors themselves, which can be estimated by Monte Carlo simulation using the known covariance matrix of fit parameters. Following a procedure qualitatively similar to that described in Sec. III, we regress to each series of satellite pairwise differences to determine the biases and target factors. From the resulting covariance matrix we generate noisy simulated sets of the fit parameters and determine trends for the merged data using these values. Sensitivities for each bias and target factor are determined by simple linear regression to the simulated trends as a function of the parameter under scrutiny. Shown in Fig. 4, the 21×21 covariance matrix from the twelve distinct satellite overlap pairs and the nine satellite target factors reveals the resulting sensitivity of regressed trends to the various overlaps and target multipliers.

The presence of large off-diagonal terms in this covariance matrix indicates that there are strong error correlations between certain parameters. In particular, due to its relatively short overlap with NOAA-07, NOAA-08, and NOAA-10, the NOAA-09 bias and target factors show up as pronounced spikes. Based on this data, we demonstrate that NOAA-09 is the weakest link in the inter-satellite merging procedure and must, therefore, be treated with great care in order to produce accurate time-series of MSU brightness temperatures.

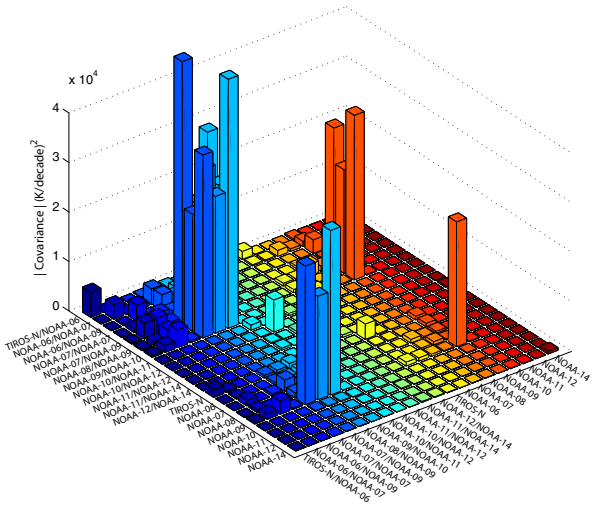

Fig. 4. The magnitude of the covariance matrix for regressed global ocean-only tropospheric temperature trends.

Acknowledgment

This work was performed with the support of the NOAA Climate and Global Change Program, Joint NOAA/NASA Enhanced Data Set Project.

References

[1] F. J. Wentz and M. C. Schabel, "Precise climate monitoring using complementary satellite data sets," *Nature,* vol. 403, pp. 414-416, 2000.

[2] F. J. Wentz and M. C. Schabel, "Effects of orbital decay on satellite-derived lower-tropospheric temperature trends," *Nature,* vol. 394, pp. 661-664, 1998.

[3] J. R. Christy, R. W. Spencer, and W. D. Braswell, "MSU Tropospheric Temperatures: Dataset Construction and Radiosonde Comparisons," *Journal of Atmospheric and Oceanic Technology,* vol. 17, pp. 1153-1170, 2000.

[4] US Space Command TLE sets are freely available online at http://www.celestrak.com.

[5] F. R. Hoots and R. L. Roehrich, "Spacetrack Report No. 3 – Models for Propagation of NORAD Element Sets," 1980.

[6] T. Mo, "A study of the microwave sounding unit on the NOAA-12 satellite," *IEEE Transactions on Geoscience and Remote Sensing,* vol. 33, pp. 1141-1152, 1995.

[7] F.J. Wentz, "Algorithm Theoretical Basis Document: AMSR Ocean Algorithm," *Remote Sensing Systems Technical Report 110398,* 1998.

[8] F. J. Wentz, M. C. Schabel, C. A. Mears, and D. Seidel, "Lower Tropospheric Air Temperature Derived from a Blended Analysis of MSU, SSM/T1, SSM/I, NCEP/NCAR Reanalysis, and Reynolds SST," *Remote Sensing Systems Technical Report 071801,* 2001.

[9] C. A. Mears, M. C. Schabel, F. J. Wentz, B. D. Santer, and B. Govindaswamy, "Correcting the MSU Middle Tropospheric Temperature for Diurnal Drifts," *IGARSS 2002 Conference Proceedings,* 2002.